the cell wall material no longer supported high CA activity. The loss of activity is not a result of acidification because material digested by 1 N HCl still supported full CA activity (Fig. 3A). The same experiment conducted with a synthetic amorphous silica (Aerosil-200), which has surface properties similar to biogenic silica (*21*), provided good buffering for CA as well. We conclude that it is the silica of diatom cell walls that is responsible for buffering rather than an organic component of the cell wall.

There is currently no protocol to purify the external CA of diatoms, so we purified the major internal CA (*22*) of *T. weissflogii* to determine the ability of biosilica to serve as a proton donor for this enzyme, which has no homology to other known CAs (*23*). The activity of this CA was high when either phosphate or biosilica was used as a buffer (Fig. 3B). Removing the buffer or using dissolved silicic acid as a buffer resulted in low catalytic rates. The lower rates observed in the SDS-cleaned frustules were a result of a lower biosilica concentration (about half the biosilica) added to the sample. The biosilica concentration was found to correlate well with CA activity (enzyme units = $0.37x$ mmol l^{-1} Si + 1.8; $P < 0.05$, $r^2 = 0.87$, n = 5 CA assays). The predicted CA activity in the absence of biosilica (1.8 enzyme units) agrees well with the observed value for incubations with no buffer (2.0 enzyme units). These results show that polymerized biosilica, unlike silicic acid, is an efficient buffer for diatom CA at the pH of seawater.

Absent a thorough understanding of the carbon acquisition systems of microalgae, it is difficult to assess the advantage that the buffering capacity of the siliceous cell wall might impart to diatoms. We note, however, that the large buffering capacity of polymerized silica would add to the energetic economy that may come from making the cell wall out of inorganic rather than organic material. This extracellular buffering may be useful for enzymatic functions other than that of CA. The necessity or usefulness of silicon in biological systems has been debated for a long time (*24*). Besides its obvious structural role, biogenic silica may well serve as a buffer in a variety of biochemical processes. It is conceivable, for example, that the documented but unexplained importance of silica in bone formation (*25*) may be linked to its role as a buffer.

In marine systems, diatoms play a major role in the export of organic carbon to the deep sea (*26*) and potentially influence the concentrations of CO_2 in the atmosphere (*27*). The last stages of the radiation of diatoms in the oceans and their dominance of the oceanic silica cycle occurred during the Eocene, about 40 million years ago (*28*). There is evidence that this is also the time when atmospheric CO_2 reached its low modern value (*29*) and organic carbon in sediments started to become enriched in ^{13}C (*30*). It is conceivable that all these phenomena are linked together mechanistically, not only because diatoms are efficient at exporting fixed CO_2 to the deep oceans but perhaps also because their siliceous cell wall makes them particularly efficient at acquiring inorganic carbon from solution.

References and Notes

1. V. Martin-Jézéquel, M. Hildebrand, M. A. Brzezinski, *J. Phycol.* **36**, 821 (2000).
2. M. Hildebrand, B. E. Volcani, W. Gassmann, J. I. Schroeder, *Nature* **385**, 688 (1997).
3. N. Kröger, R. Deutzmann, M. Sumper, *Science* **286**, 1129 (1999).
4. A. T. Davidson, D. Bramich, H. J. Marchant, A. McMinn, *Mar. Biol.* **119**, 507 (1994).
5. V. Smetacek, *Protist* **150**, 25 (1999).
6. T. A. Villareal, *Deep-Sea Res.* **35**, 1037 (1988).
7. J. A. Raven, *Biol. Rev.* **58**, 179 (1983).
8. U. Riebesell, D. A. Wolf-Gladrow, V. S. Smetacek, *Nature* **361**, 249 (1993).
9. M. R. Badger *et al.*, *Can. J. Bot.* **76**, 1052 (1998).
10. K. Aizawa, S. Miyachi, *FEMS Microbiol. Rev.* **39**, 215 (1986).
11. N. A. Nimer, M. X. Ling, C. Brownlee, M. J. Merrett, *J. Phycol.* **35**, 1200 (1999).
12. S. Burkhardt, G. Amoroso, U. Riebesell, D. Sultemeyer, *Limnol. Oceanogr.* **46**, 1378 (2001).
13. D. Sültemeyer, *Can. J. Bot.* **76**, 962 (1998).
14. Carbonic anhydrase catalyzes the hydration-dehydration reaction between CO_2 and HCO_3^- through a two-step process: a hydration-dehydration step given as $E{-}OH^- + CO_2 + H_2O \leftrightarrow E - OH_2 + HCO_3^-$ and a rate-limiting proton transfer step given as $E{-}OH_2 + B^- \leftrightarrow BH + E{-}OH^-$, where E refers to the enzyme (CA) and B refers to the buffer. The buffer then requires B^- regeneration by transfer of a proton from BH.
15. B. C. Tripp, J. G. Ferry, *Biochemistry* **39**, 9232 (2000).
16. Y. Pocker, *Cell. Mol. Life Sci.* **57**, 1008 (2000).
17. C. Tu *et al.*, *J. Am. Chem. Soc.* **123**, 5861 (2001).
18. P. Schindler, H. R. Kamber, *Helv. Chim. Acta* **51**, 1781 (1968).
19. Materials and methods are available as supporting material on *Science* Online.
20. N. Kröger, C. Bergsdorf, M. Sumper, *EMBO J.* **13**, 4676 (1994).
21. S. Dixit, P. Van Cappellen, *Geochim. Cosmochim. Acta.* **66**, 2559 (2002).
22. S. B. Roberts, T. W. Lane, F. M. M. Morel, *J. Phycol.* **33**, 845 (1997).
23. E. H. Cox *et al.*, *Biochemistry* **39**, 12128 (2000).
24. E. Epstein, *Annu. Rev. Plant Physiol. Plant Mol. Biol.* **50**, 641 (1999).
25. E. M. Carlisle, in *Silicon Biochemistry*, Ciba Symposium 121, London, 17 to 19 September 1985, D. Evered, M. O'Connor, Eds. (Wiley & Sons, Chichester, UK, 1986), pp. 123–139.
26. R. C. Dugdale, F. P. Wilkerson, *Nature* **391**, 270 (1998).
27. O. Ragueneau *et al.*, *Global Planet. Change* **26**, 317 (2000).
28. R. G. Malvia, A. H. Knoll, R. Siever, *Palaios* **4**, 519 (1989).
29. P. N. Pearson, M. R. Palmer, *Nature* **406**, 695 (2000).
30. J. M. Hayes, H. Strauss, A. J. Kaufman, *Chem. Geol.* **161**, 103 (1999).
31. We thank T. Lane for helpful discussions regarding the experimental design and M. Bender and B. Barnett for access to and assistance with mass spectrometer measurements. K. Keller, P. N. Froelich, and two anonymous reviewers provided comments which improved the manuscript. Supported by the Center for Environmental Bioinorganic Chemistry funded by NSF and DOE.

Supporting Online Material
www.sciencemag.org/cgi/content//full/297/5588/1848/DC1
Materials and Methods

11 June 2002; accepted 6 August 2002

Water Diffusion and Clustering on Pd(111)

T. Mitsui,[1] M. K. Rose,[2] E. Fomin,[2] D. F. Ogletree,[1] M. Salmeron[1]*

The adsorption, diffusion, and clustering of water molecules on a Pd(111) surface were studied by scanning tunneling microscopy. At 40 kelvin, low-coverage water adsorbs in the form of isolated molecules, which diffuse by hopping to nearest neighbor sites. Upon collision, they form first dimers, then trimers, tetramers, and so on. The mobility of these species increased by several orders of magnitude when dimers, trimers, and tetramers formed, and decreased again when the cluster contained five or more molecules. Cyclic hexamers were found to be particularly stable. They grow with further exposure to form a commensurate hexagonal honeycomb structure relative to the Pd(111) substrate. These observations illustrate the change in relative strength between intermolecular hydrogen bonds and molecule-substrate bonds as a function of water cluster size, the key property that determines the wetting properties of materials.

Intermolecular hydrogen bonds between water molecules can be comparable to or stronger than those formed between the molecule and many substrates (*1*, *2*). The relative strength of these two bonds determines the wetting properties of water. Fundamental questions regarding the adsorption of water on surfaces, from isolated molecules to clusters, complete layers, and beyond, are still unanswered. Cluster formation, including dimers and trimers at submonolayer coverage, has been analyzed by several groups using vibrational spectroscopies such as high-resolution electron energy loss spectroscopy (*3*–*7*), infrared absorption spectroscopy (*8*–*11*), and helium atom scattering (*12*). However, it is no

---

[1] Lawrence Berkeley National Laboratory, University of California, Berkeley, CA, 94720 USA. [2] Department of Physics, University of California, Berkeley, CA, 94720 USA.

*To whom correspondence should be addressed. E-mail: salmeron@stm.lbl.gov

simple task to identify clusters by purely spectroscopic means, as shown by the discrepancies in vibrational mode assignments by the different groups. Because of its atomic resolution capability, scanning tunneling microscopy (STM) can help resolve such discrepancies and can provide detailed information about the structure and dynamics of adsorbed water, from monomers to clusters and to complete layers.

Water is generally believed to form ice-like hexagonal bilayers with a $(\sqrt{3} \times \sqrt{3})R30^\circ$ periodicity on close-packed hexagonal metal surfaces (*1*, *2*, *13*, *14*), with more or less flattened rings to conform to the substrate periodicity. In a widely accepted model, this bilayer consists of H-bonded molecules, whereas a recent theoretical analysis proposes that for Ru(001) it consists instead of hexagonal rings of three water molecules and three OH groups (*15*). Low-energy electron diffraction data show a commensurate $(\sqrt{3} \times \sqrt{3})R30^\circ$ phase on Au(111) at low coverage and a compressed but oriented phase at higher coverage (*16*). Incommensurate hexagonal overlayers have been found on Pt(111) by STM (*17*, *18*).

By comparison, the structure of water below one monolayer coverage has received much less attention despite the importance of clustering and diffusion processes in wetting, hydration, and other physical and chemical interactions. STM studies have identified cyclic water hexamers at low coverage on Ag(111) (*19*) and on Cu(111) (*20*). Here we focus on the adsorption, aggregation, and diffusion of water molecules on the surface of Pd(111). By following the process of aggregation of molecules to form clusters, we have discovered that the diffusivity of small clusters (dimers, trimers, and tetramers) is several orders of magnitude above that of monomers.

The experiments were performed in an ultrahigh vacuum (UHV) chamber with a background pressure below 3×10^{-8} Pa, using a variable-temperature STM (*21*). The sample was cleaned by several cycles of noble gas bombardment at 1000 K with subsequent flashing to 1100 K. This procedure produced a clean well-ordered surface with less than 0.01% surface impurities and less than 1% subsurface impurities (*22*). Milli-Q water was used and purified by several freeze-and-pump cycles. Water was introduced into the UHV chamber via a leak valve and a dosing tube pointing toward the sample from a distance of 2 cm.

Two different techniques were used to study the diffusion of water. At high temperatures, where diffusion is fast as compared to the imaging rate, we used the atom-tracking technique, in which a feedback control in the *x-y* plane maintains the microscope tip over the molecule at all times, while its random walk motion is recorded (*23–25*). At lower temperatures, where diffusion is slow, we used movies: sequences of images acquired at ~20-s intervals in the same area. This method provides improved statistics, because many molecules can be measured at the same time.

To minimize the tip influence on the molecular motion, large gaps, low bias voltage, and low currents, typically 80 mV and 80 pA, were used. In the movie technique, the influence of the tip was found to be negligible, because during most of the image acquisition time, the tip is not over the molecule (*26*). In the atom-tracking method, the tip influence is harder to avoid because the tip is always over the molecule. Therefore, even if the interaction cross section is very small, after prolonged time in tunneling range a perturbation can occur. The tracking method was therefore used mostly in the high-temperature range, where the hopping rate is overwhelmingly determined by thermal excitation.

After adsorption at 40 K, mostly isolated water molecules were observed at low coverage. In the images they appear as maxima with a height of ~60 pm and ~0.9 nm full width at half-maximum (FWHM). The adsorption site of a molecule was determined to be on top of a Pd atom; this determination was made by comparing images acquired at high gap, which show the isolated water molecule, with images at low gap at exactly the same location, which show the Pd(111) lattice.

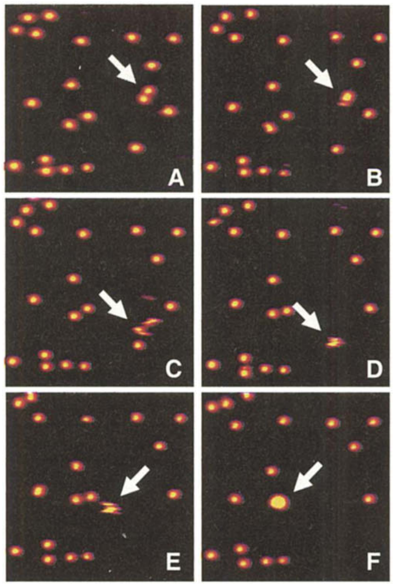

Fig. 1. Sequence of STM images showing water molecules (bright dots) adsorbed on Pd(111) at 40 K. Two monomers in (**A**) join to form a dimer in (**B**). The dimer diffuses rapidly so that the tip only scans over it for one line before moving to a nearest neighbor site, thus producing a streak in (**C**). The dimer encounters a third monomer and forms a trimer (**D**), which diffuses in (**E**), approaching a pair of nearby monomers. The arrow in (**F**) points to the pentamer formed by the collision. The scanning parameters used were as follows: 150 pA, –100 mV. Size: 180 Å × 180 Å.

Snapshots from a movie acquired at 40.0 K show several individual molecules in the form of bright dots (Fig. 1). When two nearby molecules (arrow in Fig. 1A) bind to each other (arrow in Fig. 1B), the resulting dimer diffuses very quickly, so that it only remains on site for the duration of one scan line (~120 ms) and therefore produces a streak in the image (arrow in Fig. 1C). When the dimer joins another molecule (arrow in Fig. 1D), the resulting trimer still moves faster than the monomer but slower than the dimer (arrow in Fig. 1E). The trimer comes close to two nearby monomers (Fig. 1E) and eventually merges with them to form an immobile pentamer (arrow in Fig. 1F). The clusters, in many similar sequences, were identified by observing their formation, but no internal structure could be resolved (*27*).

By measuring jump distances and directions in the movie images, diffusion was observed to proceed by random walk over nearest neighbor sites of the Pd(111) substrate. The trace of the tip in an atom-tracking experiment confirms this observation (Fig. 2). At low temperature, the rates measured by atom tracking are larger than those obtained from the movies (Fig. 3). This is due to tip influence, which is greatly enhanced by the long interaction time with the molecule during tracking (*25*). At temperatures above 52 K, however, thermal activation becomes dominant and the atom-tracking points fall on the same line as the lower temperature points acquired from movies. The activation energy barrier for water diffusion measured from this Arrhenius plot is 126 ± 7 meV, with a prefactor equal to $10^{12.0 \pm 0.6}$ Hz. This value of the energy falls between theoretical values calculated for Al(100) (*28*) (280 meV) and Pt(111) (*29*) (30 meV).

Diffusion coefficients (D_n) were obtained for several *n*-molecule clusters from STM

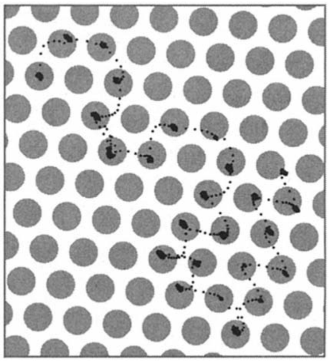

Fig. 2. Trajectory of the STM tip (the string of dots) as it tracks a water molecule in its random walk on Pd(111) at 52.4 K. A model of the Pd lattice is shown for reference. The size and orientation of the Pd lattice are known from atomic-resolution images acquired at low gap. The molecule sits on top of Pd atoms, as determined from images acquired at high and low gap, which image the molecule and the atomic lattice, respectively.

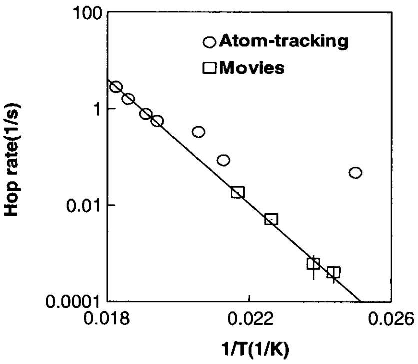

Fig. 3. Arrhenius plot of the hopping rate of a water molecule measured from STM movies (squares) and by atom tracking (circles). Below 52 K, the data from atom-tracking measurements are influenced by tip interactions and deviate from the straight line fitting the low-temperature data from movies. Above 52 K, the tip influence during tracking is negligible as compared to thermal activation. Error bars smaller than the graphic symbols are not shown.

movies at 40.0 K. Because of their rapid motion, only a lower limit of $D_2 \geq 50\ \text{Å}^2\ \text{s}^{-1}$ was obtained for dimers. For trimers, we found $D_3 = 1.02\ \text{Å}^2/\text{s}$, and we obtained an almost identical value for tetramers. The tetramers were often observed to split into two dimers. The value for monomers at this temperature is $D_1 = 2.30 \times 10^{-3}\ \text{Å}^2\ \text{s}^{-1}$, which is more than four orders of magnitude smaller than for dimers and 500 times smaller than for trimers and tetramers.

The large mobility of the small water clusters is presumably due to the combination of strong H bonding between molecules and the misfit between the O-O distance in the dimer, which is 2.96 ± 0.05 Å in the gas phase (*30–32*), and the 2.75 Å lattice constant of Pd(111). The misfit would prevent both molecules from forming bonds to the substrate in optimal geometries, thus reducing the diffusion barrier of the pair. A much smaller increase in the mobility of dimers (by a factor of two to five) has also been observed for some metal adatoms by field ion microscopy (*33*, *34*). The atoms in these metal dimers remained on similar lattice sites, however, and the observed increase was explained as the result of adatom-adatom interaction (*35*) or of exchange processes with substrate atoms (*34*). Assuming the same pre-exponential factor as for monomer diffusion, we calculate a reduction in the diffusion barrier of 27% for water dimers and 17% for trimers and tetramers. In clusters with more than four molecules, the molecules can be arranged in such a way that only alternating molecules bind directly to the substrate, whereas the rest bind to other molecules by H bonds, as in the icelike bilayers of the standard $(\sqrt{3} \times \sqrt{3})$R30° model. This arrangement should have more structural flexibility for the optimization of the molecule-surface bonds, thus reducing cluster mobility below that of isolated water molecules. An enhancement of diffusivity in small clusters due to loss of commensurability with the substrate has been predicted theoretically (*36*, *37*) in connection with the enhanced diffusion of large metallic clusters. It has also been argued that the lack of commensurability between the lattice structures of the two contacting bodies could lead to vanishing friction or superlubricity (*38*, *39*).

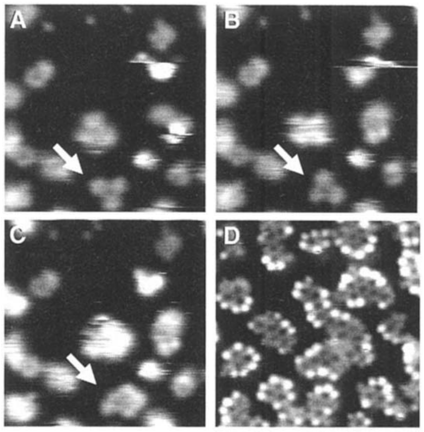

Fig. 4. Images showing clusters of various sizes and shapes on Pd(111) formed by accretion of water molecules. Changes take place as a function of time and also because of interaction with the tip. The cluster indicated by the arrow is made of three smaller clusters separated by approximately 10 Å. This cluster has rotated by 180° between (**A**) and (**B**) and is later rearranged into a set of connected hexagons in (**C**). A second cluster in (A), near the center and above the arrow, is also made of three smaller clusters. It captures more molecules and forms a four-member cluster in (B) and continues to evolve in (C). Hexagonal clusters are stable and grow into the honeycomb island structures shown in (**D**). They are made of side-sharing hexagons forming a commensurate $(\sqrt{3} \times \sqrt{3})$R30° structure. The brighter spots at the edges are water molecules presumably not yet in their final configuration. The scanning parameters used were as follows: For (A) to (C), 100 pA, 120 mV; for (D), 100 pA, 80 mV. Image size: 90 Å × 90 Å.

Clusters of various shapes and sizes form with increasing water coverage at 40 K (Fig. 4). Large clusters formed by the aggregation of smaller ones are also formed. They evolve with time, changing shape, size, and configuration until finally stable hexagonal rings are formed (Fig. 4D) (*40*). Upon further addition of water, the hexagonal rings grow into ordered honeycomb structures with $(\sqrt{3} \times \sqrt{3})$R30° periodicity relative to the Pd substrate (Fig. 4D).

Our experiments provide direct evidence of single molecular adsorption and cluster formation by successive addition of water molecules. The results demonstrate the importance of atomic-level studies in understanding the process of diffusion and growth and the enormous importance of lateral interactions.

References and Notes

1. P. A. Thiel, T. E. Madey, *Surf. Sci. Rep.* **7**, 211 (1987).
2. M. A. Henderson, *Surf. Sci. Rep.* **285**, 1 (2002).
3. H. Shi, K. Jacobi, *Surf. Sci.* **317**, 45 (1994).
4. K. Jacobi, K. Bedürftig, Y. Wang, G. Ertl, *Surf. Sci.* **472**, 9 (2001).
5. S. Andersson, C. Nyberg, C. G. Tengstål, *Chem. Phys. Lett.* **104**, 305 (1984).
6. R. Brosseau, T. H. Ellis, M. Morin, *J. Vac. Sci. Technol.* **A8**, 2454 (1990).
7. N. Materer *et al.*, *Surf. Sci.* **381**, 190 (1997).
8. M. Nakamura, M. Ito, *Chem. Phys. Lett.* **325**, 293 (2000).
9. H. Ogasawara, J. Yoshinobu, M. Kawai, *J. Chem. Phys.* **111**, 188 (1994).
10. M. Nakamura, Y. Shingaya, M. Ito, *Chem. Phys. Lett.* **309**, 123 (1999).
11. M. Nakamura, M. Ito, *Chem. Phys. Lett.* **335**, 170 (2001).
12. A. L. Glebov, A. P. Graham, A. Menzel, *Surf. Sci.* **427**, 22 (1999).
13. D. Doering, T. E. Madey, *Surf. Sci.* **123**, 305 (1982).
14. G. Held, D. Menzel, *Surf. Sci.* **316**, 92 (1994).
15. P. J. Feibelman, *Science* **295**, 99 (2002).
16. G. Pirug, H. P. Bonzel, *Surf. Sci.* **405**, 87 (1998).
17. M. Morgenstern, J. Mueller, T. Michely, G. Comsa, *Z. Phys. Chem. (Munich)* **198**, 43 (1997).
18. M. Morgenstern, T. Michely, G. Comsa, *Phys. Rev. Lett.* **77**, 703 (1996).
19. K. Morgenstern, J. Nieminen, *Phys. Rev. Lett.* **66**, 066102 (2002).
20. K. Morgenstern, K.-H. Rieder, *J. Chem. Phys.* **116**, 5746 (2002).
21. The cryogenic system was described in (*41*). The STM head used here was similar to that in (*42*), where the tip and scanner were enclosed in a copper thermal shield and were at the same temperature.
22. M. K. Rose *et al.*, *J. Chem. Phys.* **115**, 10927 (2001).
23. B. S. Swartzentruber, *Phys. Rev. Lett.* **76**, 459 (1996).
24. L. J. Lauhon, W. Ho, *J. Chem. Phys.* **111**, 5633 (1999).
25. M. Krueger, B. Borovsky, E. Ganz, *Surf. Sci.* **385**, 146 (1997).
26. At our scanning speed, the tip is within tunneling range of a molecule for about 5 ms. If the tip influences the molecular motion, the effect is easily detected by the appearance of "fractional molecules" in the images, caused by the molecule changing positions while the tip is imaging it.
27. In the images, trimer through pentamer appear somewhat larger than the monomers, with trimers ~80 to 100 pm high and pentamers ~110 pm high and slightly wider, ~1.1 nm FWHM. Dimers moved too fast to characterize.
28. J. E. Müller, J. Harris, *Phys. Rev. Lett.* **53**, 2493 (1984).
29. A. B. Anderson, *Surf. Sci.* **105**, 159 (1981).
30. S. S. Xantheas, T. H. Dunning Jr., *J. Chem. Phys.* **99**, 8774 (1993).
31. T. R. Dyke, K. M. Mack, J. S. Muenter, *J. Chem. Phys.* **66**, 498 (1977).
32. The distance between water molecules in our dimers might differ from the values in the gas phase because of interaction with the substrate.
33. K. Stolt, W. R. Graham, G. Ehrlich, *J. Chem. Phys.* **65**, 3206 (1976).
34. G. L. Kellogg, A. F. Voter, *Phys. Rev. Lett.* **67**, 622 (1991).
35. P. J. Feibelman, *Phys. Rev. Lett.* **58**, 2766 (1987).
36. P. Deltour, J.-L. Barrat, P. Jensen, *Phys. Rev. Lett.* **78**, 4597 (1997).
37. W. D. Luedtke, U. Landman, *Phys. Rev. Lett.* **82**, 3835 (1999).
38. M. Hirano, K. Shinjo, R. Kaneko, Y. Murata, *Phys. Rev. Lett.* **78**, 1448 (1997).
39. G. He, M. H. Müser, M. O. Robbins, *Science* **284**, 1650 (1999).
40. Although the triangular clusters in Fig. 4 appear similar in shape and size to the trimers reported by Morgenstern and Rieder on Cu(111) (*20*), they are interpreted differently. In our case, each component of the cluster is a smaller cluster, whereas in (*20*) the components are assigned to single water molecules separated by about four metal lattice constants.
41. S. Behler *et al.*, *Rev. Sci. Instrum.* **68**, 2479 (1997).
42. F. Mugele, Ch. Kloos, P. Leiderer, R. Moller, *Rev. Sci. Instrum.* **67**, 2557 (1996).
43. Supported by the director of the Office of Science, Office of Basic Energy Science, of the U.S. Department of Energy under contract No. DE-AC03-76SD00098. T.M. dedicates this work to Dr. L. Boesten (1935–2002).

14 June 2002; accepted 14 August 2002